Global earth mapping with NASA's Multi-angle Imaging SpectroRadiometer (MISR)

Veljko M. Jovanovic*
Jet Propulsion Laboratory, California Insitute of Technology, Pasadena, CA 91109, USA

ABSTRACT

The Multi-angle Imaging SpectroRadiometer (MISR) is a part of the payload for NASA's Terra spacecraft launched in December 1999. The MISR instrument continuously acquires a systematic, global, multi-angle imagery in reflected sunlight in order to support and improve studies of the Earth ecology and climate. This paper focuses on the photogrammetric aspect of the data production and discusses quality of the global mapping as evaluated during the first two years of the mission. Usually, remote sensing image data has been only radiometrically and spectrally corrected, as a part of standard processing, prior to being distributed to investigators. In the case of the spaceborne MISR instrument with its unique configuration of nine fixed pushbroom cameras, continuous and autonomous coregistration and geolocation of image data are required prior to application of scientific retrieval algorithm. In order to address this problem, the MISR ground data processing system includes photogrammetric processing. From the entire MISR production system, three segments can be singled out as photogrammetric in nature. These are 1) in-flight geometric calibration, 2) georectification, and 3) cloud height retrieval. The data obtained through in-flight geometric calibration significantly simplify georectification part of the standard processing. Georectification gives fundamental input to scientific retrieval including cloud-top height retrieval.
Keywords: Calibration, Geometric, Global, Mapping, Orthorectification, Photogrammetry

1. INTRODUCTION

MISR [1] is one of the five science instruments launched in December 1999, onboard the NASA's Terra spacecraft . Terra is the first in a series of the Earth Observing System (EOS) satellites intended to monitor and study the Earth ecology, climate and environment as a part of an integrated measurement approach. Data acquired by nine MISR cameras provide near-simultaneous multi-angle multi-spectral observations in order to ascertain the angular variations of reflected sunlight and the physical characteristics of the observed terrestrial scenes. The instrument and the algorithms developed to process its data represent a revolutionary approach to global remote sensing of geophysical and biophysical parameters [2]. In order to support this approach, an appropriate geometric processing is designed based on the specific accuracy requirements along with the need for unique capability of autonomous and continuous georectification. Subsequently, nine orthorectified global digital maps will be produced every nine days during the life of the mission.

The requirements for coregistration and geolocation (i.e., orthorectification), as well as stereo retrieval of a surface height from multi-temporal, multi-angle image data have been recognized since the early days of remote sensing. In order to achieve this, geometric distortions must be eliminated. In most applications with relatively high spatial resolution data, the geometric correction is not a part of standard processing. The geometric distortions are related to a number of factors, including: a) rotation of the Earth during image acquisition, b) the finite scan rate of some sensors, c) the wide field of view of some sensors, d) the curvature of the Earth, e) sensor non-idealities, f) variations in platform altitude, attitude and velocities, and g) panoramic and topographic effects related to the imaging geometry. A number of these distortions can be considered static for the life of the mission and as such removed efficiently during standard data processing. However, in many cases when the effect of a dynamically changing distortion is significant in regards to spatial resolution, the standard digital data products have only been radiometrically and spectrally corrected before being distributed to investigators, who may then need to set up an off-line geometric processing system [3]. In the case of the

* Veljko.Jovanovic@jpl.nasa.gov, phone 1 818 354-1704; fax 1 818 393-4802; 4800 Oak Grove Drive, Pasadena, CA, 91109-8099

Image and Signal Processing for Remote Sensing VIII, Sebastiano B. Serpico, Editor,
Proceedings of SPIE Vol. 4885 (2003) © 2003 SPIE · 0277/786X/03/$15.00

spaceborne MISR with its unique configuration of nine fixed pushbroom cameras, all of the above listed distortions have to be removed prior to the application of scientific retrieval algorithm. For that purpose, an algorithm based on modern digital photogrammetry methods has been implemented [4]. This paper describes operational status of an integrated process using various techniques including: a) area-based / feature-based image matching, b) image point intersection, c) space resection d) simultaneous bundle adjustment, and e) image-to-image registration. Section II describes the MISR global imaging event. Sections III and IV describe elements of the georectification process as well as current operational results.

2. GLOBAL IMAGING EVENT

2.1. Data acquisition

The Terra spacecraft is in a sun-synchronous orbit, with a baseline inclination of 98.186°. The orbit period of 98.88 minutes and orbit precession rate of 0.986°/day imply a ground repeat cycle of the spacecraft nadir point of 16 days with an equatorial local crossing time of 10:30 a.m. From the orbit altitude of about 705 km the zonal overlap swath width of MISR imaging data (that is, the swath seen by all nine cameras simultaneously along a line of constant latitude) is nominally 360 km providing multiangle coverage of the Earth in nine days at the equator and 2 days near the pole. The data in 36 spectral channels (9 cameras times four spectral bands per camera) are continuously acquired, pole-to-pole, on the dayside of the orbit. To illustrate, Figure 1 shows map projected data acquired by nadir camera during one-day period in the month of July, 2002. The cross-track instantaneous field of view and sample spacing of each pixel is 275 m for all of the off-nadir cameras, and 250 m for the nadir camera. In order to simplify manufacturing, same optical design is used for nadir and Af/Aa off-nadir cameras, resulting in slightly different cross- track instantaneous fields of view. Along-track instantaneous fields of view depend on the view angle, ranging from 250 m in the nadir to 707 m at the most oblique angle. Sample spacing in the along- track direction is 275 m in all cameras.

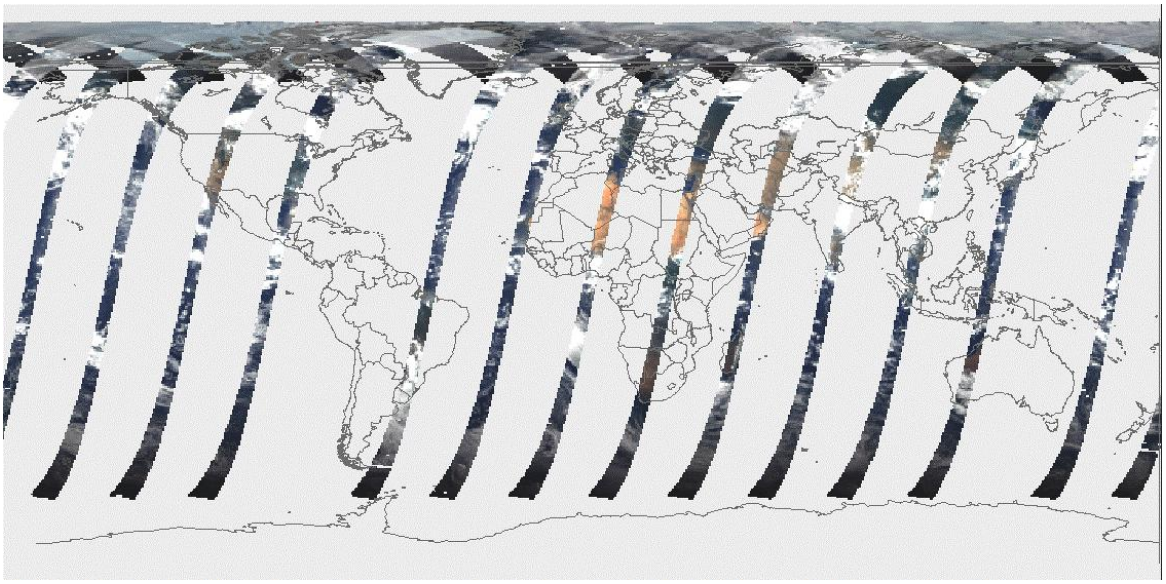

Fig. 1: The data acquired by MISR nadir camera at July 21, 2002.

2.2. Instrument geometric and radiometric characteristics

The instrument consists of nine push-broom cameras, with one camera pointing toward the nadir (designated An), one bank of four cameras pointing in the forward direction (designated Af, Bf, Cf, and Df in order of increasing off-nadir angle), and one bank of four cameras pointing in the aftward direction (using the same convention but designated Aa, Ba, Ca, and Da). Images are acquired with nominal view angles, relative to the surface reference ellipsoid, of 0°, 26.1°, 45.6, 60.0°, and 70.5° for An, Af/Aa, Bf/Ba, Cf/Ca, and Df/Da, respectively. The instantaneous displacement in the

along-track direction between the Df and Da views is about 2800 km (see Figure 1), and it takes about 7 minutes for a ground target to be observed by all nine cameras. Each camera uses four charge-coupled device line arrays parallel in a single focal plane. The line array contains 1504 photoactive pixels, each 21 μm x 18 μm. Each line array is filtered to provide one of four MISR spectral bands. The spectral band shapes are approximately Gaussian, and centered at 446, 558, 672, and 866 nm. Due to the physical displacement of the four line arrays within the focal plane of each camera, there is an along track displacement in the earth views at the four spectral bands [5]. This as well as other geometric distortions have been removed during georectification within standard ground data processing.

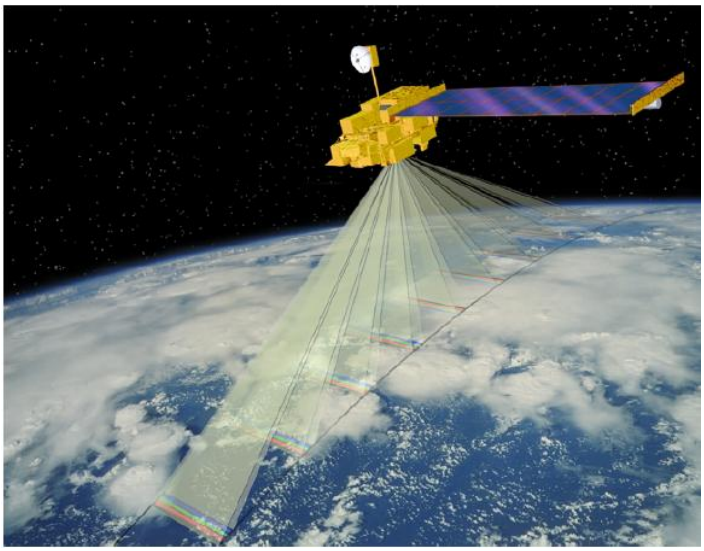

Fig 2: This graphics illustrates imaging approach of MISR instrument. Nine pushbroom cameras acquire imagery continuously during the day light portion of each orbit. The data in four spectral bands are obtained for each of nine discrete camera angles.

2.3. Virtual instrument concept

In order to meet coregistration and geolocation requirements, the multi-angle multispectral data are processed to a common map projection. We have selected Space Oblique Mercator [6] as the reference map projection grid, because it

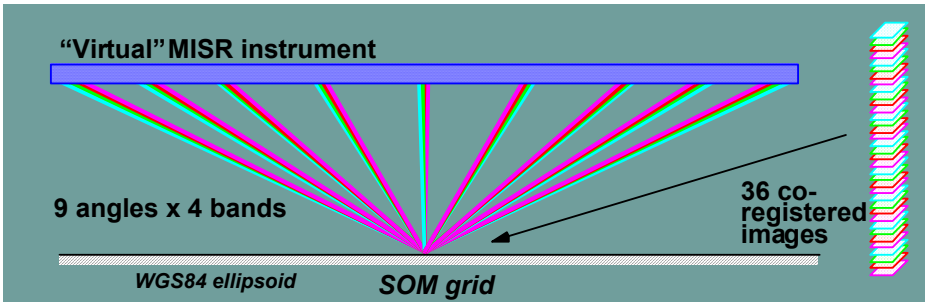

Fig. 3: Ellipsoid-projected radiance product: illustration of the acquisition by a "virtual" MISR.

is designed for continuous mapping of satellite imagery. The ground resolution of the map grid is 275 m. We define this segment of ground processing as "georectification", and the derived product as the Georectified Radiance Product. There are two basic parameters in the Georectified Radiance Product depending on the definition of the reflecting surface: a) ellipsoid-projected radiance, and b) terrain-projected radiance. The ellipsoid-projected radiance is referenced to the surface of the WGS84 ellipsoid (no terrain elevation included) and the terrain-projected radiance is referenced to the same datum including a digital elevation model over land and inland water. An ideal instrument would collect each

angular view for the terrain-projected and ellipsoid- projected radiance parameters for a ground point at the same instant, giving the radiance for each band and angle for that ground point (the so-called "virtual" MISR instrument). Naturally, the real MISR does not have these capabilities. It is up to geometric processing to produce data as if it were collected by the "virtual" MISR (compare Figure 3 to Figure 2). The spatial horizontal accuracy goal associated with these products and required by the science algorithms is an uncertainty better then ± 275 m at a confidence level of 95%. Obviously this kind of accuracy requires knowledge of a digital elevation model and removal of topographic displacements. In addition, the accuracy specifications for the supplied spacecraft navigation and attitude data suggest the possibility of horizontal errors of about 2 km in the most oblique cameras. Section III discusses the algorithms which account for all geometric displacements including removal of topography effects and errors in the spacecraft navigation data prior to the resampling of the acquired MISR imagery to the map grid.

3. AUTONOMOUS GEORECTIFICATION

3.1. Overview

In response to the specific spatial accuracy requirements, together with the need for autonomous and continuous production capabilities, we have implemented a processing strategy distributing efforts between the MISR Science Computing Facility (SCF) and the EOS [7] Distributed Active Archive Center (DAAC) in a way that minimizes the amount of processing required at the latter location. Activities at the Science Computing Facility lower the computational need at the Distributed Active Archive Center by precalculating certain datasets early in the mission and staging them for on-going use in a manner that avoids much calculation during the routine ground processing.

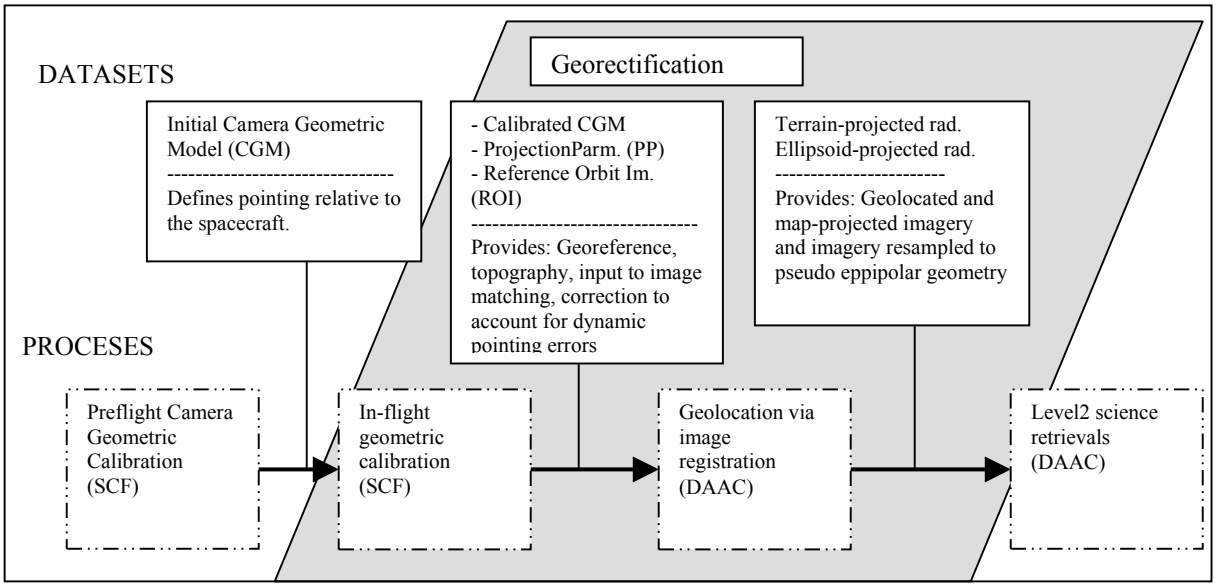

Fig. 4: Process and datasets associated with MISR georectification

These datasets include the camera geometric model, reference orbit imagery, and projection parameters. Their preparation and utilization occurred incrementally from the beginning of the mission and it is near completion. Overall process is highly computationally intensive, involving techniques such as ray casting, and matching of the different camera angles imagery. Also, significant amount of human interaction was required to test the quality of produced datasets. Consequently, routine processing of the MISR data at the (DAAC), dominated by a very high data volume, was optimized to require only the less computationally intensive work, such as registration of imagery from the same camera angle (not different camera angles) with no need for ray casting nor a high resolution digital elevation model. Figure 4 illustrates distribution of photogrammetric operations between the SCF and the DAAC.

3.2. In-flight geometric calibration

The most significant errors affecting MISR georectification and co-registration accuracy can be categorized into three groups: 1) static pointing errors, 2) dynamic pointing errors, and 3) geometric distortions due to the topography of the projection surface. The MISR in-flight geometric calibration is designed to take into account static and dynamic pointing errors. Furthermore, as a part of in-flight calibration, topographic effects are precalculated and stored to be used for the life of the mission. The calibration approach consists of two components producing two segments of the calibration dataset: 1) Camera Geometric Model (CGM), and 2) Projection Parameters (PP) and Reference Orbit Imagery (ROI).

The CGM dataset is designed to deal with static pointing errors. It consists of a set of parameters used in a mathematical expression that gives the pointing direction of an arbitrary pixel to the spacecraft attitude frame of reference. These parameters represent the geometry of the camera system and account for distortions from an ideal optical system. Some of the parameters of the camera geometric model have been calibrated during the first eight months of the mission and eventually updated based on the internal quality assessments. The calibration algorithm uses ground control points (GCPs) and focuses on the recalibration of each camera individually [8]. The objective was to isolate static and potential systematic (e.g., temperature dependent) errors of the individual cameras from the errors reported in the navigation data. This was made possible by having a large number of single camera observations of well-defined and well-distributed ground targets or GCPs. Area-based image matching [9] was used for automatic identification of GCP's.

The calibrated CGM is not sufficient to reach the required accuracy and provide foundation for on-line georectification quality assessment. This is especially true while dealing with the most oblique angles where a pointing error of 10 arcseconds will introduce a geolocation error of about 300 m. In order to routinely deal with dynamic pointing errors and facilitate automatic quality assessment, 233 pairs of PP and ROI files are being produced. A ROI file consists of cloud free MISR imagery, selected from a number of orbits passes same orbit path and mosaicked into a single image. The PP file is produced using rigorous photogrammetric methods, in order to provide accurate geolocation data for the corresponding ROI file pair. The process of creating ROI and PP pairs is similar to the regular orthorectification of time dependent imagery. A major difference is that the acquired imagery (i.e. ROI) is geolocated through PP but not resampled. A simultaneous bundle adjustment utilizing tie-points from multiangle imagery and ground control information (consisting of a global Digital Elevation Model [10] and ground control image chips [11]) is used to model dynamic errors in the supplied spacecraft navigation data.

The coupled PP and ROI files provide two major benefits to the standard georectification processing. First, expensive computation required to account for topographic displacement will be performed only once, off-line during calibration. The obtained information will be saved in a file and utilized during on-line processing throughout the mission. This is possible because of the small orbit-to-orbit variations at the same location within an orbit path, adding relatively small changes to the topographic displacements that can be accounted for in a separate process during georectification. Second, unresampled but geolocated MISR imagery will be used as ground control information. The idea is that MISR image pairs with near identical viewing geometry will provide a high success rate during least-square area-based image matching performed by standard processing during image-to-image registration

All of the planned ROI/PP production has been completed and, at the time this manuscript is being prepared for publication, a final review of the ROI is being conducted. The PP dataset have been included in the standard processing, from the beginning of the mission, successfully providing means to account for topographic distortions without need for an exhaustive computational power. Remaining ROI datasets will be utilized this fall, providing a global high accuracy ground truth dataset with regards to the overall georectification process.

3.3. Georectification within standard processing

The systematic georectification system is designed to make use of the ancillary calibration datasets from the beginning of the mission. The major information implicitly contained in these datasets is internal camera orientation, error free navigation and attitude data, georeference, and surface topography relative to the various geometries of the nine MISR cameras. This information is routinely exploited through a hybrid image registration algorithm. In particular, the autonomous and continuous georectification is reduced to a recursive image registration between ROI and new MISR imagery which consists of the following elements:

a) Image Point Intersection: a backward projection function used to provide an initial location of the conjugate points defined by the current Camera Geometric Model and supplied navigation.
b) Image matching for the precise identification of the conjugate points.
c) Transformation (mapping) function between two images.

The registration method is adaptable with regard to the character and size of misregistration, in order to minimize the processing load. The adaptive nature of the algorithm is attained by recursively dividing images into subregions until the required registration accuracy is achieved. Initially, due to the push-broom nature of the MISR cameras, subregions are rectangles extending over the image in the cross-track direction. The mapping function associated with a subregion is a modification of the affine transform, which includes known geometric characteristics of the MISR imaging event. Once the mapping between the two images is established, the last processing step is the assignment of the appropriate radiance value to the grid point of the Space Oblique Mercator map. This is achieved by using bilinear interpolation. Additional techniques are required so that autonomous production runs are unaffected by less-than-perfect input data. Some of the more obvious examples are the presence of cloudy regions, water bodies, and deserts. Such conditions significantly reduce the number of conjugate points available to determine the transformation function. In such cases supplementary procedures must be implemented. In some cases, searching for cloud-free land in the local neighborhood may be sufficient. In other cases, where a large region of data is without conjugate points, use of information obtained through the registration of the closest subregion is applied. The idea is to correct for slowly varying parameters through the use of a Kalman filter built while processing previous subregions. Also included in the algorithm is a blunder detection technique aimed at removing possible blunders coming from the image matching. This utilizes statistical results obtained from the least- square estimation of the transformation function.

4. OPERATIONAL RESULST

The MISR instrument was launched in December 1999. On February 24, 2000, the science data processing team received the first image. Soon after the initial interactive analysis and a software fix regarding band-to-band camera geometric model parameters, data acquisition for the first series of geometric calibrations started with the focus on internal pointing orientation defined by the camera geometric model.

4.1. Camera Geometric Model (CGM)

As expected, data assessment indicated no need for in-flight geometric calibration of the CGM parameters defining relative orientation of the four spectral bands within each camera. The preflight geometric calibration of the band-to-band orientation was accurate and it did not change after the launch. The band-to-band co-registration, within a camera in the Georectified Radiance Product, is better than 30 m (1σ) across all nine cameras.

At the same time, qualitative investigations regarding absolute geolocation and co-registration between nine cameras indicated that there would be large errors in both along-track (line) and across-track (sample) directions. The first step in the calibration process was to quantify errors and analyze data in order to decide which parameters of the Camera Geometric Model most probably needed adjustment. Even though the calibration algorithm and software is capable of adjustment for all parameters at the same time, a selection of a subset is recommended in order to avoid cross-correlation effects and increase redundancy and the overall robustness of least-squares estimation. For the purposes of calibration, image data acquired corresponding to 365 orbits was collected for the period April 16 through May 11, 2001. The image chips from the GCP database were matched with the acquired MISR imagery in order to identify differences between the true location and the one predicted by the Camera Geometric Model. These residuals were then plotted in a number of ways as a part of the error investigation.

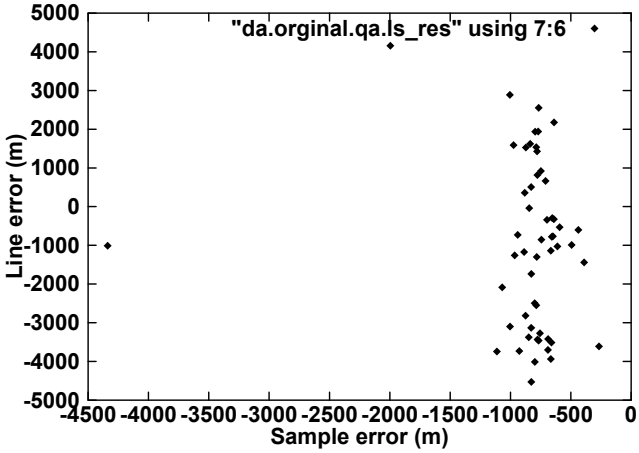

Fig 5a: Line error (along-track) plotted against sample error (across-track) for a D camera

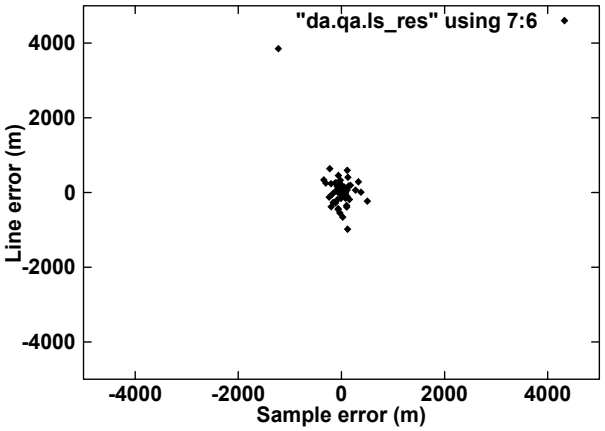

Fig 5b: Line error (along-track) plotted against sample error (across-track) for a D camera after CGM calibration

Plot in Fig 5a reveals large bias in the sample direction (roll angle) and obvious errors in other pointing parameters resulting in geolocation errors of up to 5 km in the line direction. Based on these and other graphical analyses, calibration software was configured to adjust for angles defining orientation between the camera and spacecraft attitude frame of reference. There was no indication that other CGM parameters needed adjustment. Corrections were required for all nine cameras and range between 50 arcsec to up to 1000 arcsec in some cases. Fig. 5b shows geolocation errors after static corrections to the CGM are made. At this point we reached our first goal of defining " a true static pointing knowledge of the cameras' internal geometry and orientation of the individual cameras, relative to the spacecraft attitude frame of reference". However, in order to verify static nature of the overall instrument pointing an automatic geometric quality assessment was implemented over a longer time period using georectified products obtain trough standard processing utilizing updated CGM.

4.2. Georectified radiance products

Until now standard georectification was based on only partially generated calibration datasets. Namely, so far Projection Parameters and a few versions of the Camera Geometric Model have been utilized. The generation and testing of the Reference Orbit Imagery have been completed and its inclusion into standard processing is pending final review in the fall of 2002. Consequently, current georectifed product is still affected by any type of dynamic pointing errors. To evaluate the nature and magnitude of remaining errors as well as the need for recalibration of the CGM, all of the data acquired from September 2000 to July 2001 was used. Special attention was also paid to the data surrounding in-orbit maneuvers (e.g. satellite drag makeup maneuver), as these events could affect the CGM stability. Figure 6 provide a summary of the geometric quality assessment for this 11 month time period. The detected errors in the along-track were used to estimate the mean error and standard deviation for the time segments corresponding to periods of 500 consecutive orbits. It should be noted that on the average, there were about 100 measurements per camera, per time segment. However, due to the lack of cloud free data in some cases there were too few measurements. Consequently, error estimates in those cases may be less reliable. For example, error estimates in the sample direction for the Df camera for the time period centered at orbit 4500 were made from only 15 measurements, and therefore is not considered as good as estimates for other time periods. Due to the insufficient number of error estimate measurements the time segment centered at orbit 5000 is excluded from the overall summary. Nevertheless, the results displayed in Figure 6 as well as other plots (e.g., sample direction) show that stability of the CGM and the magnitude of the geolocation errors are as expected for eight out of nine cameras. For these eight cameras, the mean errors in both directions are close to and oscillate around zero with a standard deviation within the range of 100 m up to 300 m depending on the camera view angle.

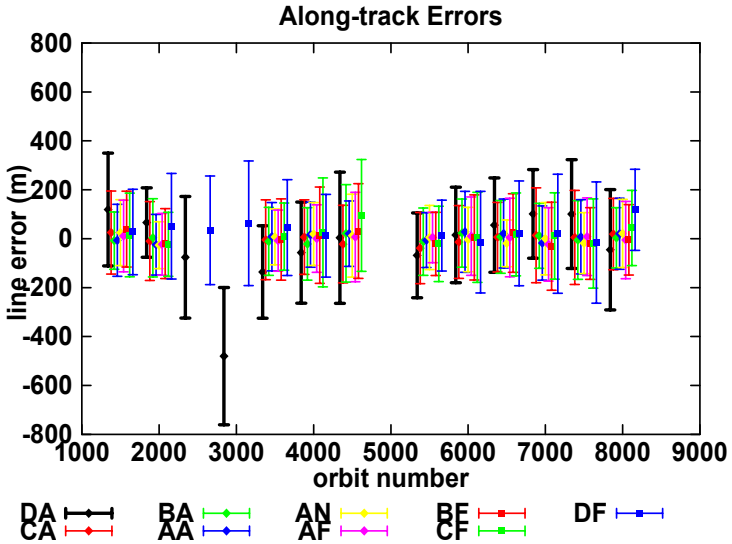

Fig 6: Along-track georectification errors as a function of time (i.e., orbit number) estimated for approximately one month (i.e. 500 orbits) time periods using a version of CGM.

These standard deviations are in agreement with the expected accuracy of image matching, used to identify ground control points, and the specified dynamic attitude errors, which are not a part of the CGM. However, the geolocation performance associated with the Da camera was not expected. Significant bias of about 300 m in the along-track and 100 m in the across-track direction has been observed since the beginning of this quality assessment. A number of attempts to recalibrate the CGM for the Da camera, using different set of parameters, or different sets of input data did not provide much better results. Further investigations focusing on the Da camera pointing reveal more cases of similar unpredictable behavior of Da camera. Nevertheless, the ROI datasets are prepared to deal with the dynamic pointing errors including non-expected issues with the Da camera.

4.3. Reference Orbit Imagery (ROI)

In addition to the unexpected un-stability of Da camera, the PP and ROI datasets are prepared to deal with any type of error with certain dynamic nature. The most prominent of those errors are contained in the attitude data. In addition to the nominal accuracy specifications of the Terra obtained attitude, significant accuracy degradation is expected during certain contact interruptions between spacecraft and TDRSS on-board navigation system. Assessments of the geolocation accuracies for one of these orbits with degraded attitude shows errors of up to 2 km (Table 1, row 2).

Cam.	Df	Cf	Bf	Af	Aa	Ba	Ca	Da	
Mean (m)	1889	808	354	74	72	290	770	1778	Without ROI
Mean (m)	376	187	88	23	76	52	232	382	With ROI

Table 1: Mean coregistration error between nadir and other eight cameras for orbit 9456 produced without and with corresponding ROI dataset.

Good thing is that only a minor percentage of all orbits are affected to this extent, and in most cases appropriate quality statements have been made visible to the user while ordering data. As a part of the creation process for ROIs, paired with existing PPs, a simultaneous bundle adjustment for nine cameras is used specifically to deal with the similar conditions as experienced in the orbit 9456. A typical output from this bundle adjustment are corrections to the instrument pointing and ephemeris modeled as the time dependent spline functions. Spline knot separations are defined based on the number

available constraint equation defined by multi-camera tie-points and estimated parameter variability. For example, Figure 7 gives cubic spline correction to a pitch angle to one of 932 orbits (4 for each of 233 orbit paths) used for generation of PP and ROI datasets.

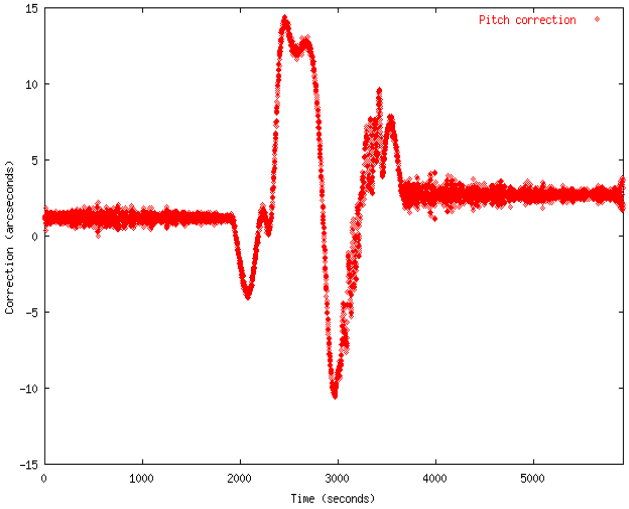

Fig. 7: Cubic spline representing pitch corrections for one of the orbits used for the creation of ROI datasets

Once ROI datasets, created for the referenced sub spacecraft trajectory corresponding to orbit 9456, are used as a part of standard processing, the mean coregistration between nine cameras is significantly improved, as shown in Table 1, row 3. As a part of the ROI testing we are conducting "global assessment" with the goal of detecting blunders in the creation ROI. MISR science processing algorithms include surface stereo height retrievals with the goal of detecting cloud heights and wind vectors [12]. These products, over clear land areas, generated with two different input configurations, are used for global testing prior to official promotion of the updated calibration dataset. A global digital elevation model [10] is also used in support of these assessments. Approach consists of evaluation of the obtained stereo height differences with the reference to the global digital elevation model. The assumption is that data produced with the ROIs should be closer to the reference, in a global sense, than the data produced without this ancillary information.

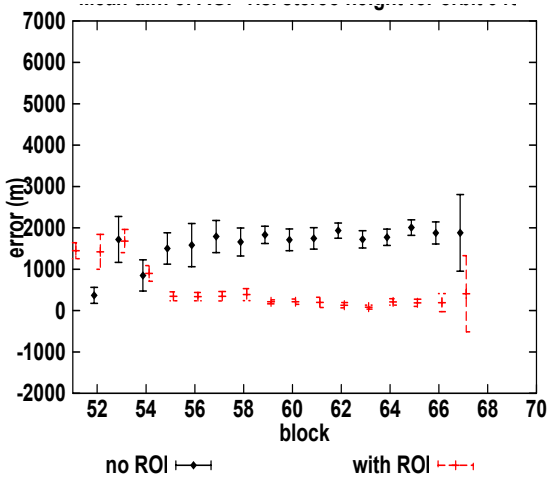

Fig. 8: Mean stereo height differences between data produced with and without ROI and a reference global digital elevation model.

It should be pointed out that in this test we are not focusing on very high accuracy evaluation. Instead, one of the driving requirements for this analysis is a complete first level quality evaluation of the 18873 files totaling 1.3 TB in size. In most cases, no significant (as defined by the thresholds of this test) differences between data produced in two configuration modes were found. Overall, as expected, there is a tendency of ROI produced data being closer to the reference. We did not detect any discrepancies indicating problems with the data tested. An example of results for the orbit cases where significant improvement is expected is given in figure 8. It can be seen that stereo heights obtained for the data produced with the PP and ROI are significantly closer to the reference for the larger part of the orbit. Discrepancies for the other part of the orbit are equally large in both cases. Interactive analysis verified that part of the orbits with no improvement is an ocean segment at the beginning of the orbit, making it not suitable for utilization of PP and ROI. As soon as there was the first piece of clear land, corrections were made and propagated further in the orbit.

4.4. Science retrievals – higher level products

As mentioned above, there are two basic parameters in the Georectified Radiance Product depending on the definition of the reflecting surface: a) ellipsoid-projected radiance, and b) terrain-projected radiance. The terrain-projected radiance is used as the input into science algorithms with focus on aerosol and surface studies. An example of using georectified multi-angle imagery to assume terrestrial angular "signatures" is given in figure 9. The geometric registration of MISR as a function of view angle enables placing data from a single spectral band at different angles into the RGB display channels.

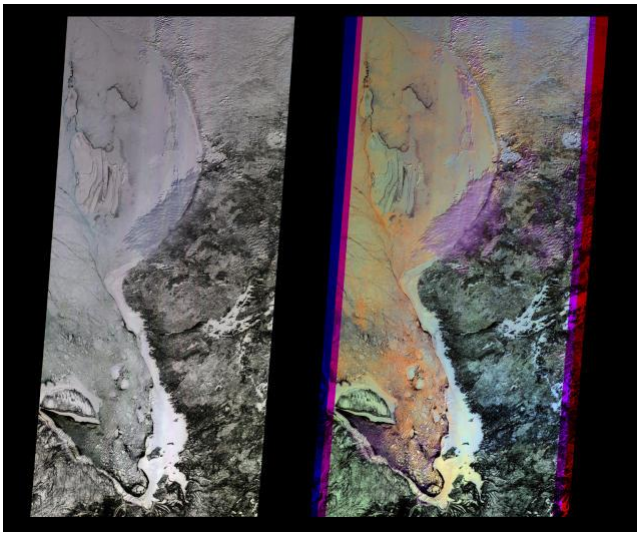

Fig. 9: Hudson Bay, Canada. Left – True color nadir georectified image. Right – Multiangle composite image.

On the left is a true-color image of Hudson Bay, Canada, area acquired with the downward-looking (nadir) camera. The false-color image on the right is a composite of red band data taken by the MISR forward 45.6-degree, nadir, and aftward 45.6-degree cameras, displayed in blue, green, and red colors, respectively. Color variations in the left image highlight spectral (true-color) differences, whereas those in the right image highlight differences in angular reflectance properties. The purple areas in the right image are low cloud, and light blue at the edge of the bay is due to increased forward scattering by the fast (smooth) ice. The orange areas are rougher ice, which scatters more light in the backward direction. So far, there is no evidence that remaining georectification errors are affecting the quality of surface and aerosol retrievals. Occasionally, some of the orbits with significant degradation in attitude accuracy are not being appropriately flagged through a manual process. With the inclusion of the ROI datasets, the autonomous quality assessment will also be a part of the standard processing to denote cases where required accuracy cannot be reached.

The ellipsoid-projected radiance is referenced to the surface of the WGS84 ellipsoid (no terrain elevation included) and as such represent multi-angle imagery of near epipolar geometry throughout the swath. It is used as the input to cloud detection, classification and characterization algorithm. In particular, MISR multiple views obtained from satellite altitude over a wide angular range provide the ability to separate the effects of cloud wind displacement from cloud height. In particular, a reference projection level known as the Reflecting Level Reference Altitude will be established

using a stereophotogrammetric algorithm. This is defined to be the level found by matching features with the greatest contrast in the near-nadir viewing directions. Physically, this corresponds to the main reflecting layer, which will typically be either the bright cloud tops or, under atmospheric conditions corresponding to clear skies or thin cloud, the surface of the earth. MISR cloud heights and winds products are being generated operationally producing very useful data especially for thick, heterogeneous cloud scenes [13]. Figure 10 gives an example of successfully retrieved height of the Hurricane Alberto over the Atlantic Ocean. However, overall improvements are expected on order to decrease blunder rate and increase global coverage area. For instance, algorithm designed to determine cloud-wind from cloud height is very sensitive to georectification accuracy, especially in regard to the most oblique D's angles. Thus, inclusion of the ROI datasets is desired in order to provide optimum input and improve success rate of cloud retrievals.

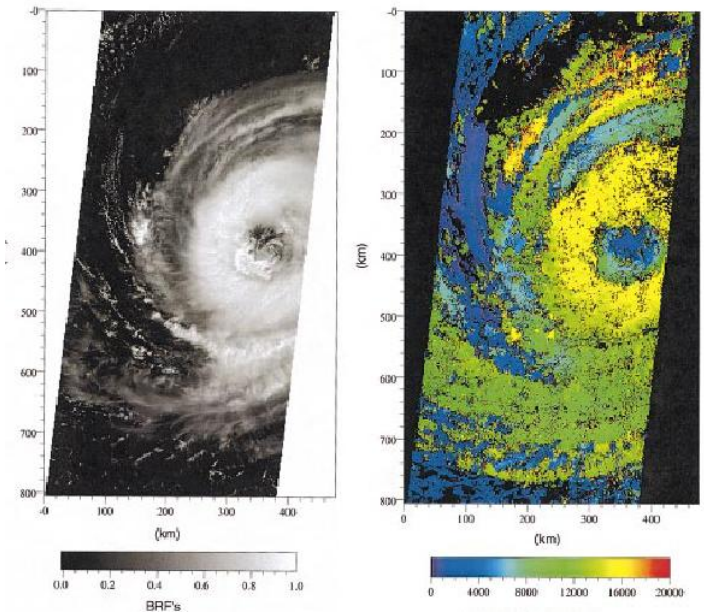

Fig. 10: Hurricane Alberto over Atlantic Ocean. Left – nadir image (red band). Right – cloud-top heights.

5. CONCLUSIONS

Data acquired by nine MISR cameras provide near-simultaneous multi-angle multi-spectral observations in order to ascertain the angular variations of reflected sunlight and the physical characteristics of the observed terrestrial scenes. The instrument and the algorithms developed to process its data represent a revolutionary approach to global remote sensing of geophysical and biophysical parameters. In order to support this approach, an integrated process based on modern photogrammetric methods has been implemented. In response to the specific spatial accuracy requirements, together with the need for autonomous and continuous production capabilities, we have implemented a processing strategy distributing efforts between the MISR Science Computing Facility (SCF) and the EOS Distributed Active Archive Center (DAAC) in a way that minimizes the amount of processing required at the latter location. In support of this strategy ancillary datasets have been produced as a result of in-flight geometric calibration effort.

Through the calibration of Camera Geometric Model we reached our initial goal of defining " a true static pointing knowledge of the cameras' internal geometry and orientation of the individual cameras, relative to the spacecraft attitude frame of reference". However, the stability of the CGM was verified for only eight out of nine cameras. The Reference Orbit Imagery datasets are prepared in order to take into account remaining pointing variability including dynamic errors in the reported spacecraft attitude and unexpected single camera instability. These datasets are being tested prior to their official promotion into the standard processing chain by the fall of 2002 in order to be ready for reprocessing of MISR data by the end of year. So far, there is no evidence that remaining georectification errors are affecting the quality of surface and aerosol retrievals in any significant number of orbits. With the inclusion of the ROI datasets, the autonomous

quality assessment will also be a part of the standard processing to denote cases where required accuracy cannot be reached. In addition, ROI datasets are desired in order to provide optimum input and improve success rate of cloud retrievals. Users can obtain MISR products [14] from the Atmospheric Sciences Data Center (ASDC) at NASA Langley Research Center, where they are generated. The ASDC [15] web site contains a great deal of information of interest to the user.

ACKNOWLEDGMENTS

The author gratefully acknowledge the efforts of the MISR Principal Investigator, D. Diner, Project Manager, G. Bothwell, Science Data System Engineer, E. Hansen, and the members of the Science Data System Team: M. Smyth, M. Bull, J. Zong, B. Rheingans, and S. Adams. Additional thanks are due to C. Moroney for her assistance in preparing cloud heights data and C. Bruegge and R. Korechoff for their efforts in pre-flight MISR camera calibration. This work was carried out at the Jet Propulsion Laboratory, California Institute of Technology, under a contract with the National Aeronautics and Space Administration. For further information, see the MISR web site at *http://www-misr.jpl.nasa.gov*.

REFERENCE

[1] D.J. Diner, J. Beckert, T. Reilly, C. Bruegge, J. Conel, R. Kahn, J. Martonchik, T. Ackerman, R. Davies, S. Gerstl, H. Gordon, J-P. Muller, R. Myneni, P. Sellers, B. Pinty, and M. Verstraete, "Multi-angle Imaging SpectroRadiometer (MISR) instrument description and experiment overview," IEEE Trans. Geosci. Rem. Sens. **36**, pp. 1072-1087, 1998.

[2] IEEE Transactions on Geoscience and Remote Sensing, "Special section on MISR" vol 40, 2002.

[3] D. Allison, M.J. Barnsley, P. Lewis N. Dyble, and J.P. Muller, "Precise geometric registration of ASAS airborne data for land surface BRDF studies, " in Proc. IGARSS, vol. 3, pp. 1655-1657, 1994.

[4] V.M. Jovanovic, M. M. Smyth, J. Zong, R. Ando, G.W. Bothwell, "MISR photogrammetric data reduction for geophysical retrievals," IEEE Trans. Goesci. Rem. Sens., 36, No. 4, 1998.

[5] J. Zong, V. M. Jovanovic, and M. M. Smyth, "MISR band-to-band registration," in Proc, SPIE, Denver, CO, vol. 2818-28, Aug. 1996.

[6] J.P. Snyder, "Map Projection-A working manual, " United States Government Printing Office, Washington, DC, United States Geological Survey Professional Paper 1395, 1987.

[7] EOS Data and Information System (EOSDIS)," EOS Reference Handbook, pp 27-35, 1999.

[8] V. Jovanovic, M. Bull, M. Smyth, and J. Zong (2002), "MISR in-flight camera geometric model calibration and achieved georectification performances," IEEE Trans. Geosci. Remote Sens., vol. 40, July 2002.

[9] F.Ackerman, "Digital image correlation: Performances and potential application in photogrammetry," Photogramm. Record, vol. 11, p. 64, 1984.

[10] T.L. Logan, EOS/AM-1 Digital Elevation Model (DEM) Data Sets: DEM and DEM Auxiliary Datasets in Support of the EOS/Terra Platform, JPL D-013508, Jet Propulsion Laboratory, California Institute of Technology, Pasadena, CA, 1999.

[11] G.B. Bailey, D. Carneggie, H. Kieffer, J.C. Storey, V.M. Jovanovic, and R.E. Wolfe, "Ground Control Points for Calibration and Correction of EOS ASTER, MODIS, MISR and Landsat 7 ETM+ Data," SWAMP GCP Working Group Final Report, USGS, EROS Data Center, Sioux Falls, SD., 1997.

[12] J. Zong, R. Davis, J.-P. Muller, and D. Diner, "Photogrammetric retrieval of cloud advection and cloud-top height from the Multi-angle Imaging Spectro-Radiometer (MISR), "Photogramm. Eng. Remote Sens., vol. 68, August 2002.

[13] C. Moroney, R. Davis, and J.-P. Muller, "Operational retrieval of cloud-top heights using MISR, "IEEE Trans. Goesci. Rem. Sens., vol. 40, July 2002.

[14] G. Bothwell, E.G. Hansen, R.E. Vargo, and K.C. Miller, "The MISR science data system, its products, tools, and performance," IEEE Trans. Geosci. Remote Sens., vol. 40, 2002.

[15] NASA Langley Research Center's Atmospheric Sciences Data Center, http://eosweb.larc.nasa.gov.

[16] E. M. Mikhail, *Observations and Least Square*. New York: Harper & Row, 1976.

[17] J.R. Wertz, Spacecraft Attitude Determination and Control. Boston: D. Reidel Publishing, 1978.